Published in final edited form as:
Cancer Res. 2012 August 1; 72(15): 3764–3774. doi:10.1158/0008-5472.CAN-11-3990.

The Oncogenic Lung Cancer Fusion Kinase CD74-ROS Activates a Novel Invasiveness Pathway Through E-Syt1 Phosphorylation

Hyun Jung Jun[1], **Hannah Johnson**[3], **Roderick T. Bronson**[4], **Sebastien de Feraudy**[5], **Forest White**[3], and **Alain Charest**[1,2,*]

[1]The Molecular Oncology Research Institute, Tufts Medical Center, Boston, MA 02111, USA

[2]Department of Neurosurgery, Tufts University School of Medicine, Boston, MA 02111, USA

[3]Koch Institute for Integrative Cancer Research, Massachusetts Institute of Technology, Cambridge, MA, 02139, USA

[4]Department of Pathology, Harvard Medical School, Boston, MA 02115, USA

[5]Department of Pathology, Brigham and Women's Hospital, Boston, MA, 02115, USA

Abstract

Patients with lung cancer often present with metastatic disease and therefore have a very poor prognosis. The recent discovery of several novel ROS receptor tyrosine kinase molecular alterations in non-small-cell lung cancer (NSCLC) presents a therapeutic opportunity for the development of new targeted treatment strategies. Here, we report that the NSCLC-derived fusion CD74-ROS, which accounts for 30% of all ROS fusion kinases in NSCLC, is an active and oncogenic tyrosine kinase. We found that CD74-ROS expressing cells were highly invasive in vitro and metastatic in vivo. Pharmacological inhibition of CD74-ROS kinase activity reversed its transforming capacity by attenuating downstream signaling networks. Using quantitative phosphoproteomics, we uncovered a mechanism by which CD74-ROS activates a novel pathway driving cell invasion. Expression of CD74-ROS resulted in the phosphorylation of the extended synaptotagmin-like protein E-Syt1. Elimination of E-Syt1 expression drastically reduced invasiveness both in vitro and in vivo without modifying the oncogenic activity of CD74-ROS. Furthermore, expression of CD74-ROS in non-invasive NSCLC cell lines readily confered invasive properties that paralleled the acquisition of E-Syt1 phosphorylation. Taken together, our findings indicate that E-Syt1 is a mediator of cancer cell invasion and molecularly define ROS fusion kinases as therapeutic targets in the treatment of NSCLC.

Introduction

ROS is an orphan receptor tyrosine kinase (RTK) proto-oncogene expressed in glioma and lung cancer (1) whose function in cancer remains unknown. Chromosomal rearrangements of the c-ROS locus that create fusion kinases have been reported in gliomas (1%) (2, 3) and cholangiocarcinomas (8.7%) (4) suggesting that ROS fusion kinases may represent a new therapeutic target.

Lung cancer is the leading cause of cancer-related deaths in the US and worldwide (5). NSCLC is a clinically challenging disease to control and in recent years, our understanding of the molecular events driving NSCLC formation and maintenance has increased

*Correspondence: Alain Charest, Tufts Medical Center, MORI, 800 Washington St, box 5609, Boston, MA, 02111. alain.charest@tufts.edu, 617-636-8876 (phone), 617-636-5277 (Fax).

No potential conflicts of interest were disclosed.

dramatically, leading to changes in the treatment of this disease where targeted therapy against activated kinases can be an effective and successful approach (6). The majority of NSCLC patients are diagnosed with advanced stage that spread beyond the primary site and approximately half of patients have metastatic (stage IV) disease at diagnosis thus limiting treatment options to palliative management (7). The extent of the invasive component seen in lung cancer is strongly associated with clinical outcomes. Patients presenting with non-invasive tumors, which are biologically indolent, have a much better prognosis than those with adenocarcinomas, a highly invasive tumor with increased risk of metastatic disease and death. As invasion is an early step of cancer metastasis, a detailed understanding of the molecular mechanisms of tumor cell invasion is required to provide new treatment options.

Using split FISH BAC assays to screen for ROS gene rearrangements, two groups recently reported that approximately 1.4% of NSCLCs harbor ROS rearrangements, defining a new genetic subtype of NSCLC (8, 9). The authors identified known and novel fusion partners for ROS and to date, ROS fusion partners are TPM3, SDC4, SLC34A2, LRIG3, CD74 and EZR with the most common event reported being CD74-ROS. With an estimated >200,000 new cases of lung cancer per year in the U.S. alone, there are approximately 3,000 new ROS-rearranged NSCLC tumors per year (10). In both studies, the authors found that ROS fusion-positive patients tend to be younger, never-smokers with a histologic diagnosis of adenocarcinoma presenting with stage IV disease (8, 9).

Here we report that the NSCLC ROS fusion kinase CD74-ROS, similar to FIG-ROS, is highly oncogenic. We provide evidence that pharmacological inhibition of ROS fusion kinases produces anti-tumorigenic effects and we observed that CD74-ROS expressing cells are highly invasive compared to FIG-ROS positive cells. We uncovered the molecular mechanism driving this invasiveness using phosphoproteomics. We report that E-Syt1, an extended synaptotagmin-related C2-domain containing protein, is highly phosphorylated (Y993) in CD74-ROS expressing cells and that elimination of E-Syt1 expression abolishes invasion of these cells both in vitro and in vivo. Our results uncover a function for E-Syt1 in the transduction of invasive signals in cancer cells.

Materials and Methods

ROS fusion constructs, retrovirus production and transformation assays

The various ROS fusion constructs depicted in Fig. 1A were assembled using standard molecular biology techniques as detailed in Supplementary Materials and Methods. The cDNAs were expressed using the pLXSN retrovirus system (11) produced in Phoenix cells (Gary Nolan, Stanford University) and used to infect Rat1 or NSCLC cells as described (12). Monoclonal cell lines were isolated by selecting individual G418-resistant colonies and assayed for density saturation growth, colony formation assays, growth in soft agar and migration assays as described in detail in Supplementary Materials and Methods and elsewhere (2).

Immunoprecipitation and immunoblotting

Target proteins were immunoprecipitated as follows: cells were lysed by resuspension in lysis buffer (2). The lysates were incubated for 10 min on ice and the cell debris was pelleted by centrifugation. The indicated antibodies were added to the supernatants along with protein A/G-agarose beads (Invitrogen), and binding was allowed to proceed for 16 hr at 4°C. The bead-bound protein complexes were washed before being subjected to SDS-PAGE. Western blots were performed as follows: cell lysates were prepared as above and total cell lysates were separated on polyacrylamide gels and transferred to a PVDF membrane (Immobilon P, Millipore). Blots were blocked for 1 hour and primary antibodies

were added to the blocking solution and incubated overnight at 4°C on a shaker. Blots were washed several times and then the secondary antibodies were incubated for 1 hour followed by several washes and enhanced chemiluminescence (ECL) reactions were performed as described by the manufacturer (Western Lightning Kit, Perkin Elmer).

Growth in immunocompromised mice

All animal procedures were performed in accordance with Tufts University's recommendations for care and use of animals and were maintained and handled under protocols approved by IACUC. Assays of tumorigenicity in immunocompromised mice were performed as previously described (13). Briefly, 5×10^6 of the indicated cells were injected subcutaneously in PBS or matrigel and tumor growth was monitored over time using caliper measurements.

Sample preparation, phosphopeptide immunoprecipitation, labeling and MS

Clonal Rat1 cells expressing the indicated ROS fusion proteins were incubated for 24 h in serum-free media then lysed and differentially labeled with 8plex. Instrumentation settings and reagents are described in details in the Supplementary Materials and Methods.

RNA interference

RNAi-mediated knockdown was performed using the lentiviral pSicoR-pgkPURO vector system (14). Five short hairpin sequences were designed using the pSICOLIGOMAKER 1.5 software against rat E-Syt1 mRNA sequence and cloned, along with a scrambled sequence control shRNA, into pSicoR-pgkPURO according to established protocols (http://web.mit.edu/jacks-lab/protocols/pSico.html). Lentiviruses were prepared as described elsewhere (14) and used to infect Rat1 CD74-ROS cells followed by selection with puromycin (4 μg/mL). Individual clones were selected and expanded for analysis.

Statistical analysis

Statistical analyses were performed using the two-tailed, unpaired Student's t test in Prism 5.0 (GraphPad Software).

Results

Oncogenic activity of ROS fusion kinases

We have previously demonstrated the oncogenic activity of FIG-ROS both in vitro and in vivo (2, 3, 15). Here, we sought to validate the oncogenic activities of the newly described NSCLC-derived CD74-ROS and SLC34A2-ROS fusion kinases. Using standard molecular biology techniques, we recreated the CD74-ROS and two isoforms of the SLC34A2-ROS fusion cDNAs and expressed these, along with FIG-ROS, in immortalized, non-transformed Rat1 cells (Fig. 1A). After selection, clonal isolates were screened for expression levels and kinase activity by immunoblots (Supplementary Fig. 1A) and three clones for each constructs demonstrating similar expression levels and kinase activity were chosen for transformation studies.

Expression of kinase active (WT) forms of FIG-ROS and CD74-ROS but not SLC34A2-ROS proteins in Rat1 cells led to a drastic change in cellular morphology, which correlated with their capacity to reach elevated saturation densities (Fig. 1B). Expression of active CD74-ROS and FIG-ROS can overcome saturation-dependent growth arrest in Rat1 cells in a focus formation assay. Foci were not observed with their kinase-inactive versions (KM), vector (pLXSN) control or from the SLC34A2-ROS expressing cells (Fig. 1C and Supplementary Fig. 1B). Cells expressing FIG-ROS-WT and CD74-ROS-WT are capable of

sustained growth in an anchorage-independent environment whereas control cell lines and cells expressing SLC34A2-ROS were incapable of growing under the same conditions (Fig. 1D and Supplementary Fig. 1C). To further examine their tumorigenicity, FIG-ROS and CD74-ROS expressing cells were injected subcutaneously into immunocompromised mice. FIG-ROS or CD74-ROS expressing cells developed tumors with a relatively short latency (20–25 days) whereas no tumors were found in mice injected with cells expressing kinase-inactive versions, pLXSN vector control or SLC34A2-ROS (Fig. 1E). Finally, we demonstrated that CD74-ROS and FIG-ROS are capable of conferring enhanced migratory potential to cells in an in vitro “scratch” assay (Supplementary Fig. 1D). Together, these results demonstrate that FIG-ROS and CD74-ROS fusion kinases are oncoproteins. Surprisingly, SLC34A2-ROS lacks transformation potential under identical circumstances, suggesting perhaps that localization or signaling differences between SLC34A2-ROS and FIG-ROS or CD74-ROS might be responsible for this observation.

Distinct cellular localization and signaling of ROS fusion kinases

CD74 and SLC34A2 are integral plasma membrane-spanning proteins. To determine the cellular localization of CD74-ROS and SLC34A2-ROS, we performed indirect immunofluorescence microscopy. Unlike FIG-ROS, which is a Golgi apparatus-associated oncoprotein (2), the staining pattern of CD74-ROS and SLC34A2-ROS in Rat1 cells advocate that these fusion kinases reside within the plasma membrane (Supplementary Fig. 2A). Furthermore, CD74-ROS and SLC34A2-ROS co-localized with the plasma membrane marker epidermal growth factor receptor (EGFR). These results were validated by subcellular fractionation studies that demonstrated that CD74-ROS and SLC34A2-ROS proteins are present within plasma membrane fractions (Supplementary Fig. 2B).

Next, we ascertained whether these differences in localization affect the signaling profiles of these kinases. Studies on ROS signaling demonstrated that ROS activates SHP-1 and SHP-2, ERK1/2, IRS-1, PI3K, AKT and STAT3 signaling pathways (1). We performed western blot analysis using phospho-specific antibodies against known ROS target signaling pathways and showed that expression of FIG-ROS and CD74-ROS but not their kinase-inactive counterparts nor SLC34A2-ROS activates the MAPK, SHP-2, STAT-3, Akt and mTORC1 pathways (Supplementary Fig. 3A–D). These results demonstrate that although SLC34A2-ROS localized to the plasma membrane and is an active kinase, it is incapable of stimulating signaling pathways that are common between FIG-ROS and CD74-ROS and known to be oncogenic.

ROS fusion kinases are potential therapeutic targets

The amino acid sequence of the kinase domain of ROS is highly homologous to that of the ALK RTK. We hypothesized that ROS fusion kinase-expressing cells would be sensitive to the tool compound ALK inhibitor NVP-TAE684 (16) and the clinical compound Crizotinib (PF-02341066) (17). Treatment of FIG-ROS or CD74-ROS cells with NVP-TAE684 led to a dose dependent reduction in growth with IC_{50} values of less than 10 nM (Fig. 2A). This reduction in growth parallels the inhibition of the kinase activity of ROS fusion kinases (Supplementary Fig. 4A) and an attenuation of their signaling networks (Fig. 2B). To validate ROS fusion kinases as genuine therapeutic targets, we evaluated the activity of NVP-TAE684 on the transformation capacity of ROS fusion kinases. We performed experiments on cell growth, saturation-dependent growth inhibition and anchorage-independent growth assays on FIG-ROS and CD74-ROS expressing Rat1 cells in the presence of vehicle control or 10 nM of NVP-TAE684 (Fig. 2C-E and Supplementary Fig. 4B) and showed that inhibition of ROS fusion kinases has drastic anti-cancer effects on these cells. Treatment of cells expressing FIG-ROS or CD74-ROS with the clinically available drug Crizotinib led to a dose dependent reduction in growth with IC_{50} values of

less than 5 nM (Supplementary Fig. 4C). Finally, we evaluated the effects of a recently described ROS-specific kinase inhibitor; KIST301080 (18, 19) and determined that the optimal concentrations of this compound for ROS kinase inhibition is relatively high (10–50 μM) (Supplementary Fig. 5A–E), and was not pursued further. Taken together, these results demonstrate that small-molecule based inhibition of ROS fusion kinase activity with an inhibitor is a potent anti-oncogenic treatment that can reverse the transformed phenotype of these cancer cells.

CD74-ROS expressing cells are highly invasive and metastatic

Histopathological analysis of FIG-ROS and CD74-ROS Rat1 xenograft tumors revealed that CD74-ROS tumors are more invasive than those derived from FIG-ROS, capable of infiltrating through the parietal peritoneum, extraperitoneal fat and muscle layers (Fig. 3A) and observed to metastasized to lymph nodes (Fig. 3B). This difference in invasiveness between FIG-ROS and CD74-ROS is also observed in vitro in a matrigel Boyden chamber invasion assay (Fig. 3C). CD74-ROS expressing cells are 15.8 fold more invasive than vector control cells whereas FIG-ROS expressing cells are 1.6 fold more invasive than control cells. These results demonstrate that expression of CD74-ROS in Rat1 cells triggers a mechanism that renders cells highly invasive and metastatic.

Quantitative phosphotyrosine profiling of FIG-ROS, CD74-ROS and SLC34A2-ROS expressing Rat1 cells

We surmised that the observed difference in invasiveness between FIG-ROS and CD74-ROS expressing cells might be due to potential differences in the activation of tyrosine phosphorylation signaling pathways. We performed a quantitative phosphoproteomics analysis across kinase active and kinase dead versions of FIG-ROS, CD74-ROS, SLC34A2-ROS and vector control Rat1 cells. Quantitative analysis of 3 biological replicates yielded 89 phosphotyrosine peptides identified and quantified in 2 or more analyses. The mean ratio for each peptide was calculated along with the standard deviation and coefficient of variation across biological replicates (the complete dataset is summarized in Table S1). To identify the phosphotyrosine sites that are specifically associated with CD74-ROS-WT expressing Rat1 cells, and thus the invasive phenotype, we compared the relative iTRAQ intensities of signals observed in the FIG-ROS-WT and the CD74-ROS-WT expressing Rat1 cells. Of the 89 phosphotyrosine peptides, 35 were significantly different with an associated p value of ≤ 0.05 (Fig. 4A). This list of significantly different tyrosine phosphorylated peptides was then sorted based on those with the greatest relative intensity in the CD74-ROS-WT expressing cells. E-Syt1 phosphorylation on site pY993 was found to be the most highly increased in CD74-ROS-WT compared to FIG-ROS-WT expressing cells (Fig. 4B,C). The observed increase in tyrosine phosphorylation of E-Syt1 was validated by immunoprecipitation western using lysates from vector control, FIG-ROS-WT and CD74-ROS-WT expressing Rat1 cells (Fig. 4D). The increase in phosphorylation at pY993 appears to be due to an increase in the upstream signaling pathways, as the E-Syt1 protein levels remains constant across pLXSN, CD74-ROS-WT and FIG-ROS-WT cells (Fig. 5A).

E-Syt1 mediates CD74-ROS-triggered invasiveness

To solidify the role of E-Syt1 in conferring increased invasiveness in CD74-ROS expressing cells, we used RNAi to knock down the expression of E-Syt1 in these cells. Two potent E-Syt1 shRNAs and a scrambled sequence control shRNA were chosen to create clonally selected cell lines from Rat1 cells expressing FIG-ROS, CD74-ROS and from vector control Rat1 cells (Supplementary Fig. 6A,B). We performed invasion assays and demonstrated that E-Syt1 knockdown CD74-ROS expressing cells no longer invade in vitro (Fig. 5B) and in vivo when grown subcutaneously as xenograft tumors (Fig. 5C). These results demonstrate that expression of CD74-ROS confers invasiveness to cells through the activity of E-Syt1.

We confirmed that the loss of invasiveness was not due to a loss of oncogenic activity from CD74-ROS by performing growth curves, colony formation assays and growth in soft agar assays and growth of xenograft using CD74-ROS cells and E-Syt1 knockdown cells. We demonstrated that elimination of E-Syt1 does not affect the ability of CD74-ROS to transform cells (Supplementary Fig. 6C–G). The effects of eliminating E-Syt1 expression on the activation of ROS signaling networks parallel those on cell transformation, that is, loss of E-Syt1 had no effect on the signaling of MAPK, SHP-2, STAT-3, Akt and mTORC1 pathways (Supplementary Fig. 7A–D). These results demonstrate that eliminating the expression of E-Syt1 in CD74-ROS expressing cells abolished the invasiveness of these cells without affecting the oncogenic transformation capacity of CD74-ROS.

To validate these results in a model of NSCLC, CD74-ROS was expressed in three non-invasive NSCLC cell lines (NCI-H1915, NCI-H2009 and NCI-H1755) and three independent clones for each construct were selected for in vitro invasion studies (Fig. 6A). Expression of CD74-ROS in the H1915, H1755 and H2009 lines induced invasion 18.4, 13.3 and 3.5 fold over control vector cells respectively (Fig. 6B). Expression of kinase inactive CD74-ROS was incapable of conferring invasive properties to the same cells. Similar to the Rat1 cells, the acquisition of an invasive phenotype parallel the appearance of phosphorylated E-Syt1 in CD74-ROS expressing cells (Fig. 6A). Lastly, we ascertained the ROS canonical signaling networks in NSCLC lines stably expressing CD74-ROS. Unlike the Rat1 cell model, only SHP-2 is activated in all three lines whereas the MAPK, mTORC1 and STAT-3 pathways are moderately engaged or absent (Fig. 7A,B).

Discussion

In recent years, our understanding of the molecular events driving NSCLC formation and maintenance has increased dramatically, fueling paradigm shifts in treatment of this disease. The subdivision of NSCLC into clinically relevant molecular subsets according to specific driver mutations led to seminal trials for NSCLC patients with mutant EGFR treated with gefitinib that resulted in a prolonged progression-free survival and an improved quality of life when compared to patients given only cytotoxic chemotherapy (20, 21). Similarly, the EML4-ALK fusion kinase defines a second clinically actionable oncogenic driver mutation in NSCLC that yielded a similarly impressive response rate (22). Two recent large-scale screens for ROS fusion kinases in NSCLCs have revealed that 1.4% of NSCLC have rearrangements at the c-ROS locus, which defines a new molecular subclass of NSCLC. Of the ROS fusion positive tumors, 30% are known to harbor a recurrent translocation *t*(5;6)(q32;q22), which creates the CD74-ROS fusion kinase described herein.

The advent of large-scale molecular genetic studies of cancer such as the ones described above, continues to uncover a significant number of mutations in various genes. Although the results of many these events appear a priori to be oncogenic, there is a requirement for empirical validation of their oncogenicity in controlled paradigms. Our studies demonstrate that CD74-ROS, like FIG-ROS, is a potent oncoprotein capable of readily transforming fibroblast cells through activation of the canonical signaling pathways SHP-2, STAT-3 and MAPK. Surprisingly, in the same context, the SLC34A2-ROS fusion kinase was unable to activate these pathways and is incapable of transformation even though its tyrosine kinase activity is comparable to that of CD74-ROS and FIG-ROS. This lack of oncogenicity for SLC34A2-ROS is similar to results recently reported by Takeuchi and colleagues (9) and suggests that cellular transformation by SLC34A2-ROS might be context dependent.

Our results suggest that CD74-ROS represents a new target for the treatment of NSCLC. The high degree of homology between the kinase domains of ALK and ROS predicts that ALK inhibitors would exert inhibition of ROS. Indeed, we demonstrated that the ALK

inhibitor tool compound NVP-TAE684 and the clinically available ALK/MET inhibitor Crizotinib displayed low IC_{50} values against ROS fusion kinases expressing cells and showed that pharmacological inhibition of ROS fusion kinases results in compelling anti-cancer effects. In fact, while this manuscript was under review, our results were validated in a NSCLC patient afflicted with a ROS fusion kinase positive tumor who displayed a remarkable response to Crizotinib treatment (8).

So far, CD74-ROS has only been observed in NSCLC (8, 9, 23). Although parallels can be inferred and new pathways can be discovered from fibroblast expression models of cancer (as seen in the current study), they often constitute a weak alternative to cancer-specific derived models. Because there are no established NSCLC cell lines that endogenously express CD74-ROS, we relied on ectopic expression of CD74-ROS in non-invasive NSCLC lines to study the effects of CD74-ROS kinase activity on signaling and invasion. Using three non-invasive NSCLC lines (H1915, H2009 and H1755), we demonstrated that expression of active CD74-ROS drastically causes these cells to invade and that the invasion parallels the appearance of E-Syt1 phosphorylation on tyrosine residues. These results are similar to our earlier observations in fibroblasts and demonstrate that in a clinically relevant context, expression of CD74-ROS induces invasive mechanisms that likely rely on E-Syt1 activity.

Interestingly, ectopic expression of CD74-ROS in established NSCLC tumor cell lines triggers variable signaling responses. The canonical MAPK, STAT-3 and mTORC1 pathways are utilized to various degrees in these lines, from non-existent to moderate. This likely result from the fact that the tumors that gave rise to these lines arose under specific combinations of tumor suppressor genes loss and oncogenes activation (other than CD74-ROS) and are thus “wired” a certain way. This “wiring” may or may not express signaling members that are canonical to an ectopically expressed oncoprotein (e.g. CD74-ROS). In this context ectopic expression of an oncogenic protein (e.g. CD74-ROS) may display variable signaling responses when presented to different tumor cell lines. One consistent signaling response to ROS fusion kinase expression however is the activation of SHP-2, a known oncoprotein, which we observed both in fibroblasts and in all three NSCLC cell lines. It is therefore likely that the major driving signaling pathway initiated by ROS fusion kinases is the activation of SHP-2.

Although FIG-ROS and CD74-ROS are equally oncogenic, we discovered that CD74-ROS expressing cells displayed an invasive and metastatic phenotype over FIG-ROS cells. Lymph node metastasis is rarely seen in xenograft models, underlying the strength of CD74-ROS signaling as pro-invasive and metastatic. We surmised that differences in phosphorylation of downstream targets might be responsible for this observation and a global quantitative phosphoproteomic screen revealed that the plasma membrane protein E-Syt1 is 16 times more phosphorylated on Y993 in CD74-ROS expressing cells than in FIG-ROS cells. By eliminating E-Syt1 expression in CD74-ROS cells the invasive phenotype was abrogated in vivo and in vitro. This reduction of expression did not affect the activation of the signaling pathways SHP-2, STAT-3 and MAPK nor did it affect CD74-ROS oncogenicity. It is conceivable that localization of FIG-ROS to the Golgi membrane prevents access to E-Syt1, whereas CD74-ROS, a plasma membrane-bound receptor, readily has access to E-Syt1.

E-Syt1 is a member of the E-Syt family (E-Syt1-3) (24) of membrane proteins structurally composed of an NH_2-terminal transmembrane region, a highly conserved intracellular juxtamembrane domain and five (E-Syt1) or three (E-Syt2 and E-Syt3) COOH-terminal C2 domains (24, 25). C2 domains are protein modules that generally act as Ca^{2+}- and phospholipid-binding domains and/or as protein-protein interaction domains (26). E-Syt1 is

assumed to be an integral plasma membrane protein given its overall architecture although Min et al., have demonstrated that transiently overexpressed E-Syt1 in HEK293 cells localizes to endomembranes (24). Regardless of its localization, our results demonstrate that E-Syt1 is phosphorylated on Y993 in plasma membrane-bound CD74-ROS expressing cells and not in Golgi apparatus located FIG-ROS expressing cells.

Tyrosine 993 resides within the fifth C2 domain of E-Syt1 and is conserved amongst other E-Syt family members. The same C2 domain has been demonstrated in E-Syt2 to be required for E-Syt2 plasma membrane binding (24). It is conceivable that phosphorylation on Y993 in E-Syt1 may modulate a similar C2-mediated plasma membrane association, which may be important for the regulation of E-Syt1 function in cancer cell invasion. Phosphorylation of E-Syt1 on tyrosine sites has been observed in various cancers. Phosphorylation on Y832 has been detected in breast cancer MCF-10A cells expressing CSF-1R (27), in PYK2 expressing NIH-3T3 cells (28), in stomach cancer MKN-45 cells treated with the MET inhibitor SU-11274 (29, 30) and the NSCLC cells H3255 treated with gefitinib (29, 30) and H1703 treated with imatinib (30). It has also been detected in human mammary epithelial cell (HMEC) (31) and Jurkat cells (32). Phosphorylation of E-Syt1 on Y1019 (homologue of Y993 in rat) has also been detected in 32D cells expressing both plasma membrane and endoplasmic reticulum bound activated Flt3 RTK (33), in MKN-45 cells (29) and in numerous NSCLC human biosamples (23). It is unlikely that CD74-ROS is present in all those different cancer cell types and biosamples, suggesting that alternative events can promote the phosphorylation of E-Syt1. Our results suggest that phosphorylated E-Syt1 may confer invasiveness and metastatic potential to cancer cells and offer a new therapeutic strategy against cancer cell invasion and metastasis.

Supplementary Material

Refer to Web version on PubMed Central for supplementary material.

Acknowledgments

This work was supported, in whole or in part by the National Cancer Institute grant U01CA141556 (A.C., F.W.) and the American Cancer Society Research Scholar Grant 117409 (A.C.). We would like to thank Drs. Ken Hung for critical review of the manuscript, Gary Nolan (Stanford University, Stanford, CA) for the Pheonix packaging cells and Ibrahim El-Deeb (University of Science and Technology, Daejeon, Republic of Korea) for the KIST301080 compound.

References

1. Acquaviva J, Wong R, Charest A. The multifaceted roles of the receptor tyrosine kinase ROS in development and cancer. Biochim Biophys Acta. 2009; 1795:37–52. [PubMed: 18778756]
2. Charest A, Kheifets V, Park J, Lane K, McMahon K, Nutt CL, et al. Oncogenic targeting of an activated tyrosine kinase to the Golgi apparatus in a glioblastoma. Proc Natl Acad Sci U S A. 2003; 100:916–21. [PubMed: 12538861]
3. Charest A, Lane K, McMahon K, Park J, Preisinger E, Conroy H, et al. Fusion of FIG to the receptor tyrosine kinase ROS in a glioblastoma with an interstitial del(6)(q21q21). Genes Chromosomes Cancer. 2003; 37:58–71. [PubMed: 12661006]
4. Gu TL, Deng X, Huang F, Tucker M, Crosby K, Rimkunas V, et al. Survey of tyrosine kinase signaling reveals ROS kinase fusions in human cholangiocarcinoma. PLoS One. 2011; 6:e15640. [PubMed: 21253578]
5. Herbst RS, Heymach JV, Lippman SM. Lung cancer. N Engl J Med. 2008; 359:1367–80. [PubMed: 18815398]
6. Lovly CM, Carbone DP. Lung cancer in 2010: One size does not fit all. Nat Rev Clin Oncol. 2011; 8:68–70. [PubMed: 21278771]

7. Howlader, N.; Noone, AM.; Krapcho, M.; Neyman, N.; Aminou, R.; Waldron, W., et al. SEER Cancer Statistics Review, 1975–2008. National Cancer Institute; Bethesda, MD: 2011. http://seer.cancer.gov/csr/1975_2008/, based on November 2010 SEER data submission, posted to the SEER web site, 2011
8. Bergethon K, Shaw AT, Ignatius Ou SH, Katayama R, Lovly CM, McDonald NT, et al. ROS1 Rearrangements Define a Unique Molecular Class of Lung Cancers. J Clin Oncol. 2012; 30:863–70. [PubMed: 22215748]
9. Takeuchi K, Soda M, Togashi Y, Suzuki R, Sakata S, Hatano S, et al. RET, ROS1 and ALK fusions in lung cancer. Nat Med. 2012; 18:378–81. [PubMed: 22327623]
10. Janne PA, Meyerson M. ROS1 Rearrangements in Lung Cancer: A New Genomic Subset of Lung Adenocarcinoma. J Clin Oncol. 2012; 30:878–9. [PubMed: 22215755]
11. Miller AD, Rosman GJ. Improved retroviral vectors for gene transfer and expression. Biotechniques. 1989; 7:980–2. 4–6, 9–90. [PubMed: 2631796]
12. Kriegler, M. Gene Transfer and Expression: A Laboratory Manual. Oxford University Press; USA: 1993.
13. Bookstein R, Shew JY, Chen PL, Scully P, Lee WH. Suppression of tumorigenicity of human prostate carcinoma cells by replacing a mutated RB gene. Science. 1990; 247:712–5. [PubMed: 2300823]
14. Ventura A, Meissner A, Dillon CP, McManus M, Sharp PA, Van Parijs L, et al. Cre-lox-regulated conditional RNA interference from transgenes. Proc Natl Acad Sci U S A. 2004; 101:10380–5. [PubMed: 15240889]
15. Charest A, Wilker EW, McLaughlin ME, Lane K, Gowda R, Coven S, et al. ROS fusion tyrosine kinase activates a SH2 domain-containing phosphatase-2/phosphatidylinositol 3-kinase/mammalian target of rapamycin signaling axis to form glioblastoma in mice. Cancer Res. 2006; 66:7473–81. [PubMed: 16885344]
16. Galkin AV, Melnick JS, Kim S, Hood TL, Li N, Li L, et al. Identification of NVP-TAE684, a potent, selective, and efficacious inhibitor of NPM-ALK. Proc Natl Acad Sci U S A. 2007; 104:270–5. [PubMed: 17185414]
17. Timofeevski SL, McTigue MA, Ryan K, Cui J, Zou HY, Zhu JX, et al. Enzymatic characterization of c-Met receptor tyrosine kinase oncogenic mutants and kinetic studies with aminopyridine and triazolopyrazine inhibitors. Biochemistry. 2009; 48:5339–49. [PubMed: 19459657]
18. El-Deeb IM, Park BS, Jung SJ, Yoo KH, Oh CH, Cho SJ, et al. Design, synthesis, screening, and molecular modeling study of a new series of ROS1 receptor tyrosine kinase inhibitors. Bioorg Med Chem Lett. 2009; 19:5622–6. [PubMed: 19700314]
19. Park BS, El-Deeb IM, Yoo KH, Oh CH, Cho SJ, Han DK, et al. Design, synthesis and biological evaluation of new potent and highly selective ROS1-tyrosine kinase inhibitor. Bioorg Med Chem Lett. 2009; 19:4720–3. [PubMed: 19596575]
20. Mok TS, Wu YL, Thongprasert S, Yang CH, Chu DT, Saijo N, et al. Gefitinib or carboplatin-paclitaxel in pulmonary adenocarcinoma. N Engl J Med. 2009; 361:947–57. [PubMed: 19692680]
21. Rosell R, Moran T, Queralt C, Porta R, Cardenal F, Camps C, et al. Screening for epidermal growth factor receptor mutations in lung cancer. N Engl J Med. 2009; 361:958–67. [PubMed: 19692684]
22. Kwak EL, Bang Y-J, Camidge DR, Shaw AT, Solomon B, Maki RG, et al. Anaplastic lymphoma kinase inhibition in non-small-cell lung cancer. N Engl J Med. 2010; 363:1693–703. [PubMed: 20979469]
23. Rikova K, Guo A, Zeng Q, Possemato A, Yu J, Haack H, et al. Global survey of phosphotyrosine signaling identifies oncogenic kinases in lung cancer. Cell. 2007; 131:1190–203. [PubMed: 18083107]
24. Min SW, Chang WP, Sudhof TC. E-Syts, a family of membranous Ca2+-sensor proteins with multiple C2 domains. Proc Natl Acad Sci U S A. 2007; 104:3823–8. [PubMed: 17360437]
25. Morris NJ, Ross SA, Neveu JM, Lane WS, Lienhard GE. Cloning and preliminary characterization of a 121 kDa protein with multiple predicted C2 domains. Biochim Biophys Acta. 1999; 1431:525–30. [PubMed: 10350628]

26. Cho W, Stahelin RV. Membrane binding and subcellular targeting of C2 domains. Biochim Biophys Acta. 2006; 1761:838–49. [PubMed: 16945584]
27. Knowlton ML, Selfors LM, Wrobel CN, Gu TL, Ballif BA, Gygi SP, et al. Profiling Y561-dependent and -independent substrates of CSF-1R in epithelial cells. PLoS One. 2010; 5:e13587. [PubMed: 21049007]
28. Bonnette PC, Robinson BS, Silva JC, Stokes MP, Brosius AD, Baumann A, et al. Phosphoproteomic characterization of PYK2 signaling pathways involved in osteogenesis. J Proteomics. 2010; 73:1306–20. [PubMed: 20116462]
29. Guo A, Villen J, Kornhauser J, Lee KA, Stokes MP, Rikova K, et al. Signaling networks assembled by oncogenic EGFR and c-Met. Proc Natl Acad Sci U S A. 2008; 105:692–7. [PubMed: 18180459]
30. Moritz A, Li Y, Guo A, Villen J, Wang Y, MacNeill J, et al. Akt-RSK-S6 kinase signaling networks activated by oncogenic receptor tyrosine kinases. Sci Signal. 2010; 3:ra64. [PubMed: 20736484]
31. Heibeck TH, Ding SJ, Opresko LK, Zhao R, Schepmoes AA, Yang F, et al. An extensive survey of tyrosine phosphorylation revealing new sites in human mammary epithelial cells. J Proteome Res. 2009; 8:3852–61. [PubMed: 19534553]
32. Mayya V, Lundgren DH, Hwang SI, Rezaul K, Wu L, Eng JK, et al. Quantitative phosphoproteomic analysis of T cell receptor signaling reveals system-wide modulation of protein-protein interactions. Sci Signal. 2009; 2:ra46. [PubMed: 19690332]
33. Choudhary C, Olsen JV, Brandts C, Cox J, Reddy PN, Bohmer FD, et al. Mislocalized activation of oncogenic RTKs switches downstream signaling outcomes. Mol Cell. 2009; 36:326–39. [PubMed: 19854140]

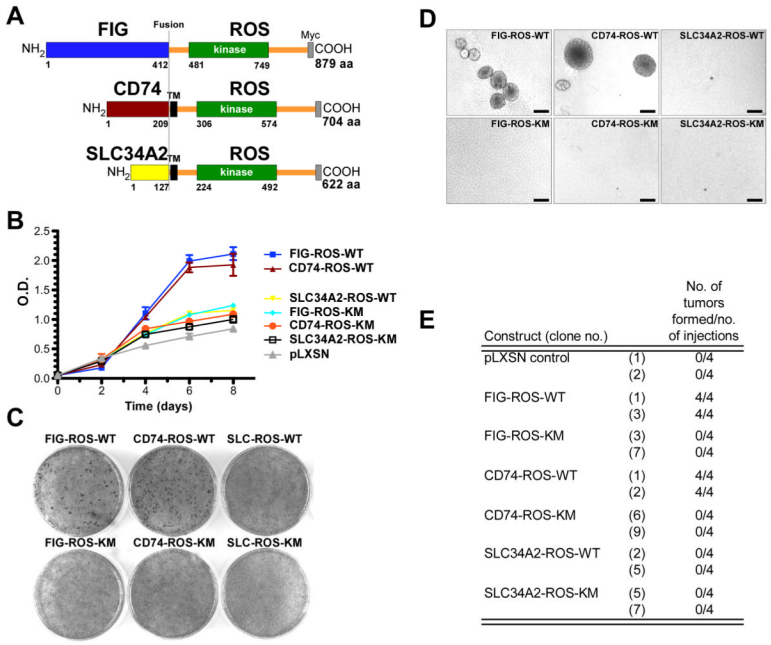

E

Construct (clone no.)		No. of tumors formed/no. of injections
pLXSN control	(1)	0/4
	(2)	0/4
FIG-ROS-WT	(1)	4/4
	(3)	4/4
FIG-ROS-KM	(3)	0/4
	(7)	0/4
CD74-ROS-WT	(1)	4/4
	(2)	4/4
CD74-ROS-KM	(6)	0/4
	(9)	0/4
SLC34A2-ROS-WT	(2)	0/4
	(5)	0/4
SLC34A2-ROS-KM	(5)	0/4
	(7)	0/4

Figure 1.

ROS fusion kinases are oncogenic. A, schematic representation of the ROS fusion kinases used in this study. The numbering refers to the amino acid position for the indicated domains of the fusion proteins. All constructs are Myc epitope tagged. B, growth curves of ROS fusion kinases expressing Rat1 clones. For each indicated ROS fusion construct, results from three independent clones are averaged and plotted as the mean ± S.D. Representative photographs of Rat1 cells expressing the indicated ROS fusion kinase variants in (C) focus formation and (D) anchorage-independent growth in soft agar assays. Quantitation of the focus formation assay is depicted in Supplementary Fig. 1B. E, growth of the indicated ROS fusion expressing Rat1 clones as subcutaneous xenografts in immunocompromised mice. 10^6 Rat1 cells were injected into the flanks of $NIH^{nu/nu}$ mice and tumors developed within 20–25 days. Mice that did not developed tumors were observed for a period of 50 days. Kinase-inactive (KM) versions of these ROS fusions proteins were included as controls. The construct SLC34A2-ROS is abbreviated to SLC-ROS. Scale bar= 250 μm.

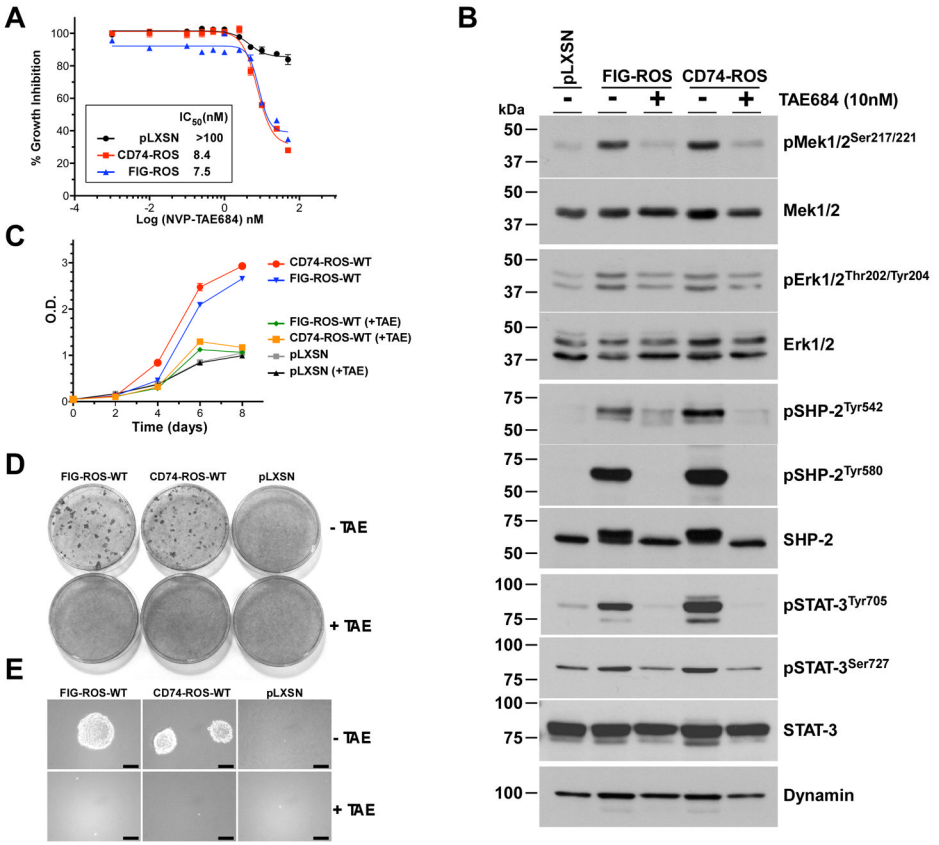

Figure 2.

Cells expressing ROS fusion kinases are sensitive to ALK inhibitors. A, ROS fusion kinases-expressing Rat1 cells were grown in the presence of NVP-TAE684 to determine IC_{50} values. B, western blot analysis of total cell lysates from pooled Rat1 clones of ROS fusion kinases treated with NVP-TAE684 for 24 hours and probed for the indicated signaling proteins using phospho-specific antibodies. Blots were stripped and rehybridized with the indicated antibodies to control for expression levels and loading. (C–E) NVP-TAE684 reverses ROS fusion kinase-expressing Rat1 cells transformed phenotype. Cells were treated with NVP-TAE684 (10 nM) or vehicle and assayed for (C) saturation density growth inhibition, (D) focus formation and (E) growth in soft agar. Quantitation of the focus formation assay is depicted in Supplementary Fig. 4B.

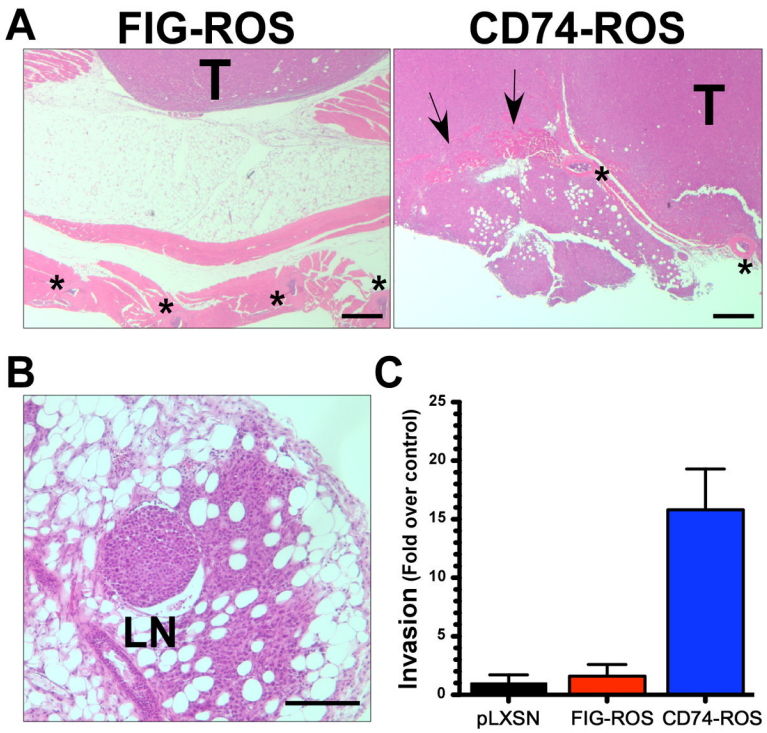

Figure 3.

CD74-ROS expressing cells are highly invasive and metastatic. (A, B) Representative photomicrographs of H&E stained paraffin embedded cross sections of subcutaneous xenograft tumors from clonal FIG-ROS and CD74-ROS expressing Rat1 cells. Arrows point to invasive areas. Stars mark the locations of ribs. T; tumor, LN; lymph node. Scale bars: (A) 500 μm (B) 250 μm. C, graphical representation of CD74-ROS invasiveness as measured by in vitro Boyden chamber matrigel invasion assays.

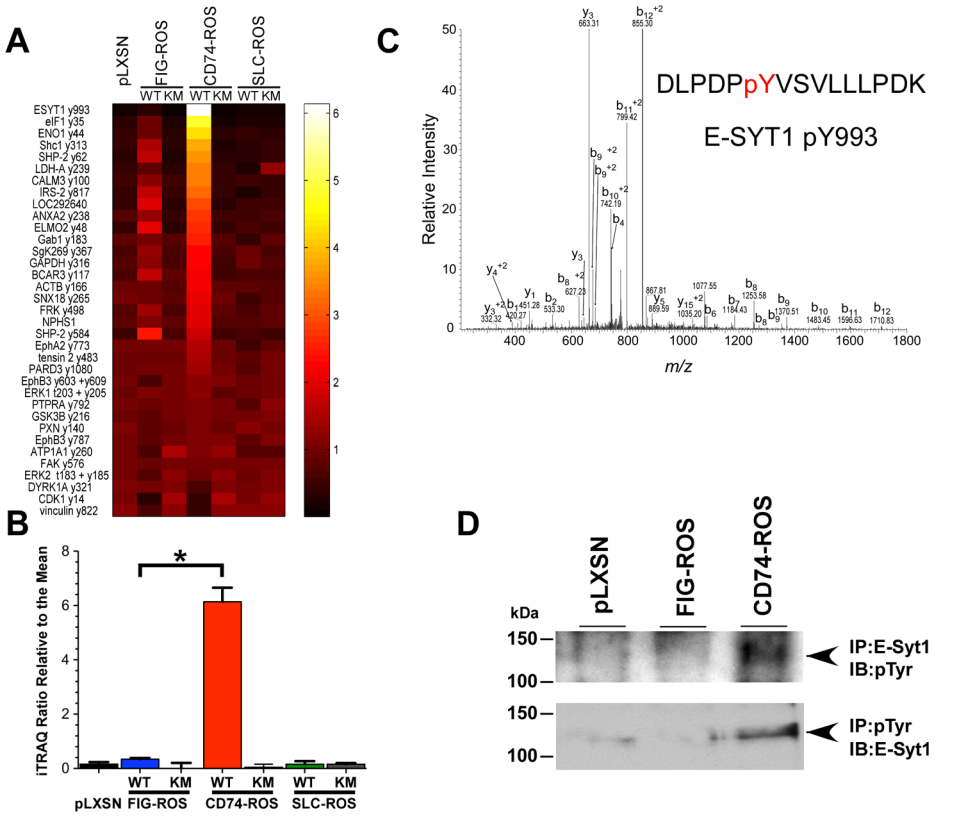

Figure 4.

Quantitative phosphotyrosine profiling reveals significant differences between FIG-ROS and CD74-ROS expressing Rat1 cells. A, thirty five tyrosine phosphorylated peptides that were found to have significantly different ($p=\leq 0.05$) levels between FIG-ROS and CD74-ROS expressing cells are represented in a heat map. Peptides were sorted based on the relative iTRAQ ratios found in CD74-ROS relative to the mean. Protein names are abbreviated and phosphorylation site numbering is based on that present in phosphosite. SLC34A2-(S)ROS expressing cells are abbreviated as SLC-ROS. Ratios shown on the axis refer to iTRAQ ratios relative to the mean. B, bar chart depicting the relative iTRAQ ratios across 3 biological replicates. Error bars are representative of the standard deviation. FIG-ROS-WT and CD74-ROS-WT ratios are significantly different based on students t-test. * $p=2.07\ e^{-5}$. C, a representative manually validated tandem MS spectrum of E-SYT1 peptide DLPDPYVSVLLLPDK indicating the presence of phosphorylation site pY993 (mascot score; 37). D, lysates from parental Rat1 cells (pLXSN vector control), FIG-ROS and CD74-ROS expressing cells were immunoprecipitated (IP) with either E-Syt1 or anti phosphotyrosine antibodies. The immunoprecipitates were analyzed for phosphotyrosine content (pTyr) or for the presence of E-Syt1 protein respectively by immunoblotting (IB).

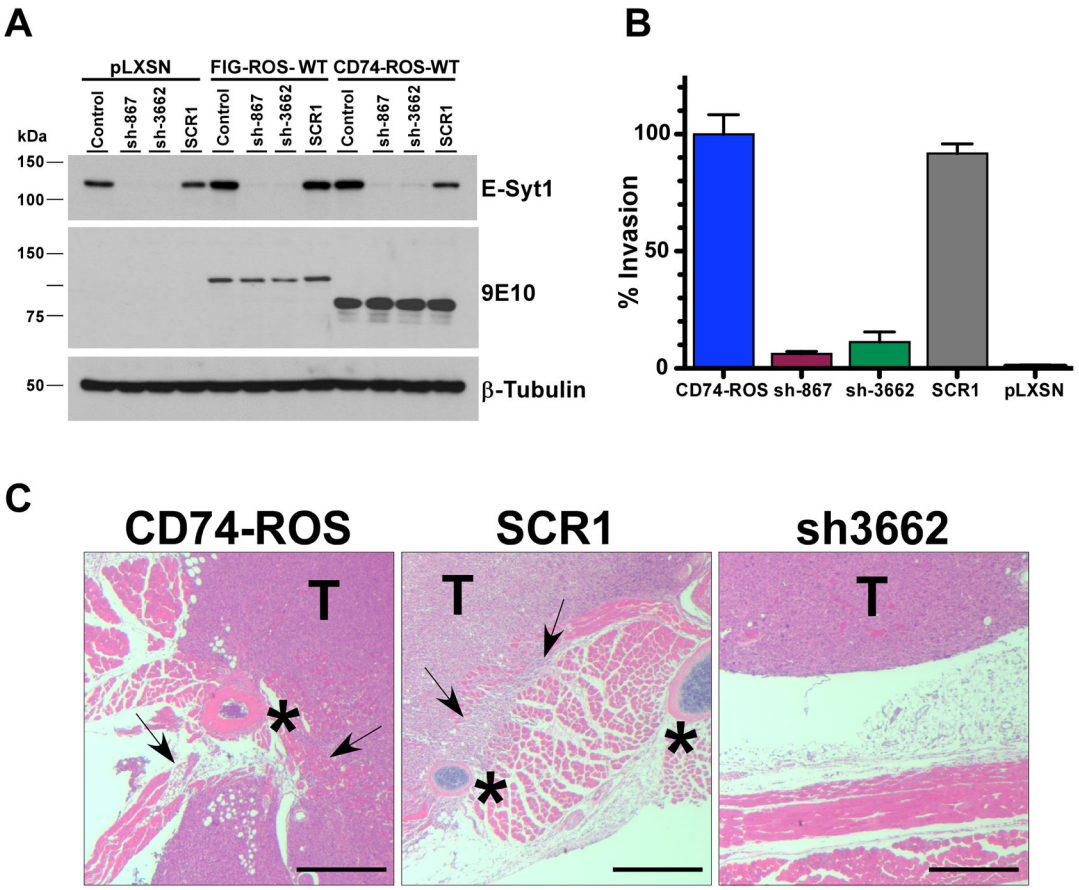

Figure 5.

E-SYT1 is a driver of invasion. A, western blot analysis of E-Syt1 expression knock down from control pLXSN, FIG-ROS and CD74-ROS expressing Rat1 cells using a scrambled control and two short hairpin RNAs. B, graphical representation of the in vitro invasiveness of parental CD74-ROS expressing Rat1 cells and E-Syt1 shRNA knock down clones and controls. C, elimination of E-Syt1 expression in CD74-ROS Rat1 cells abolishes invasion in vivo. Arrows point to invasive areas. Stars mark the locations of ribs. T; tumor. Scale bar: 500 μm.

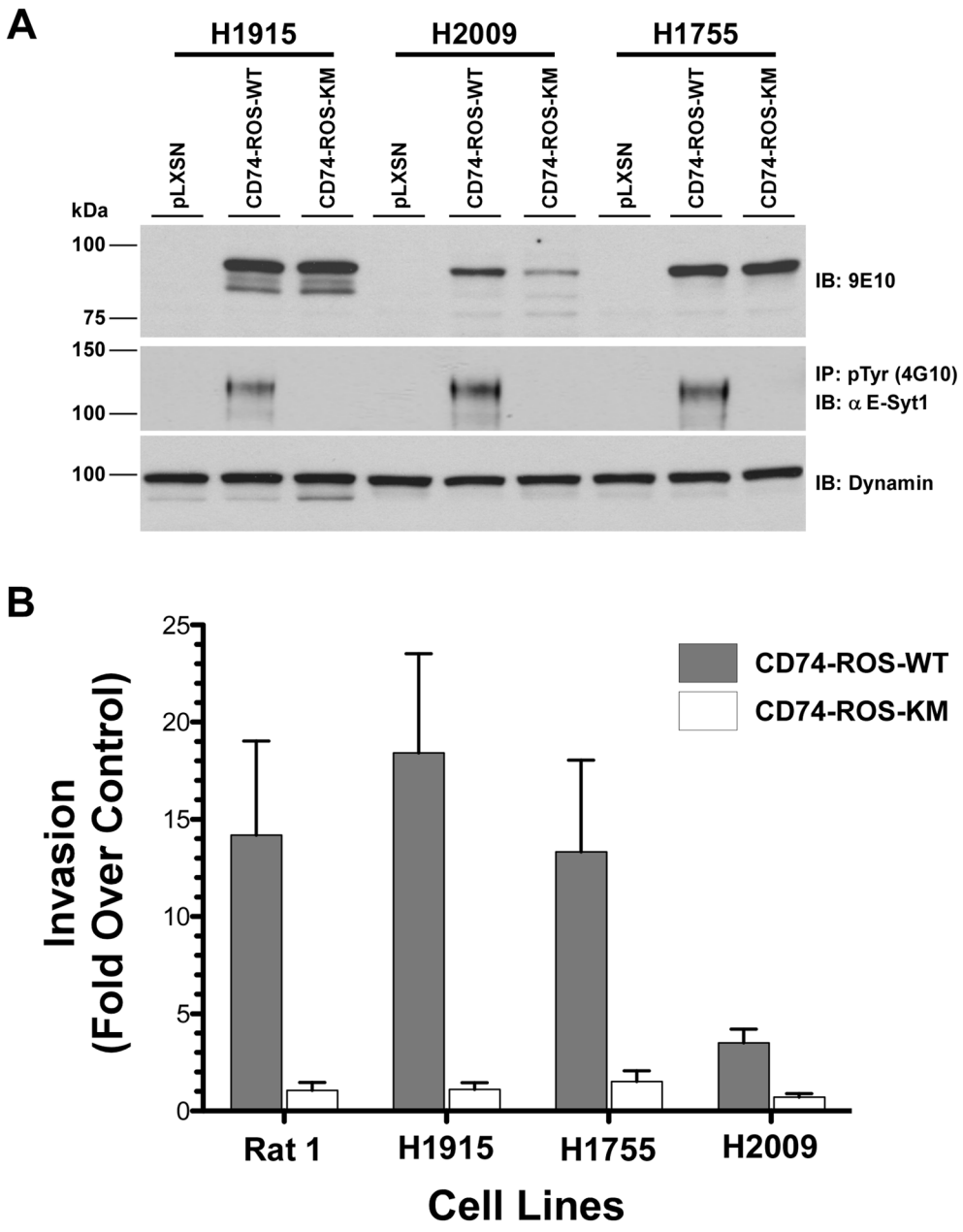

Figure 6.

Expression of CD74-ROS in NSCLC cells induces invasion and E-Syt1 phosphorylation. A, cell lysates from the indicated NSCLC cell lines expressing CD74-ROS-WT or CD74-ROS-KM fusion proteins were immunoblotted for expression levels (9E10) and immunoprecipitated (IP) with an anti phosphotyrosine antibody and analyzed for the presence of E-Syt1 protein by immunoblotting (IB). B, graphical representation of in vitro invasion of NSCLC cell lines expressing CD74-ROS-WT or CD74-ROS-KM fusion proteins. The data is shown as fold increase in invasion when compared to empty pLXSN vector controls for the respective lines and is calculated using three independent clones for each construct.

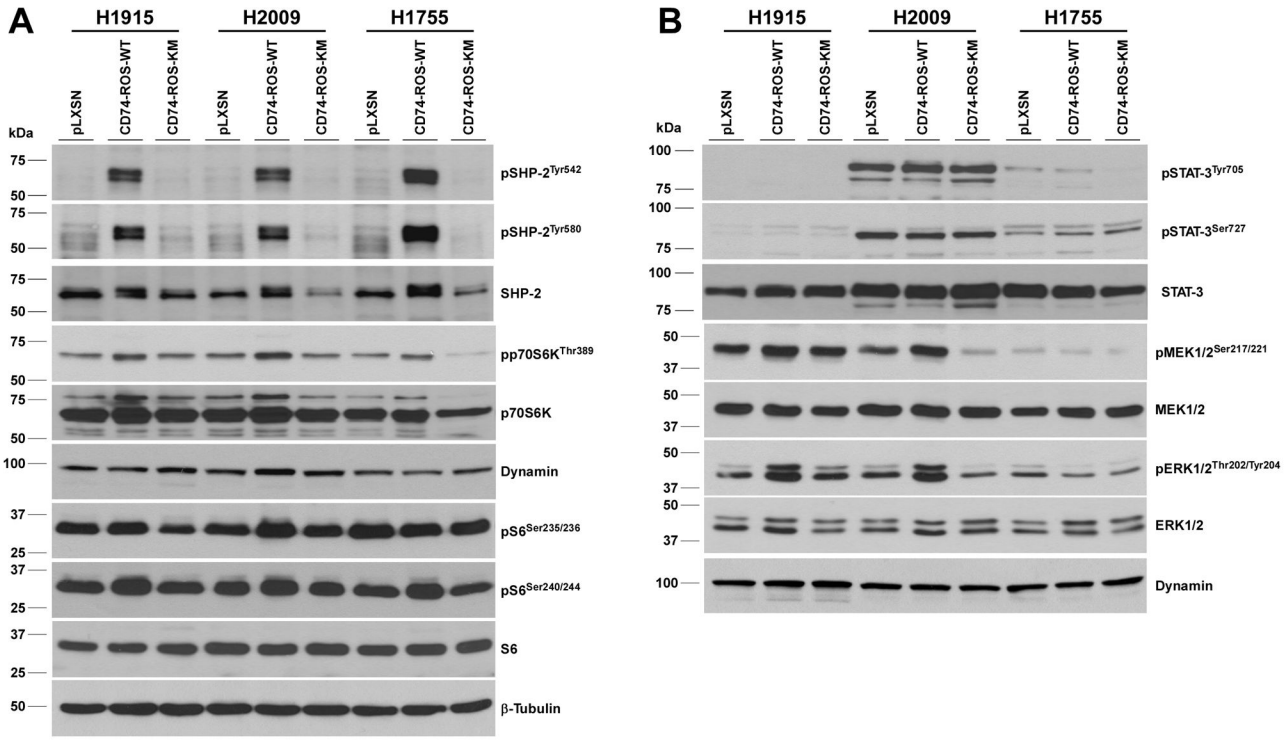

Figure 7.

Expression of CD74-ROS in NSCLC cells induces SHP-2 signaling. Immunoblot analysis of total cell lysates from pools of three independent NSCLC clones from each of the NSCLC cell lines probed for the indicated proteins using phospho-specific antibodies. A, activation of the tyrosine phosphatase SHP-2 and the mTORC1 pathways. B, the STAT-3 and MAPK pathways. All blots were stripped and rehybridized with the indicated antibodies to control for expression levels and loading.